# Phase determination by wavelength-modulated diffraction. I. Centrosymmetric case

**T. Koganezawa, Y. Yoshimura, N. Nakamura and H. Iwasaki***

*Faculty of Science and Engineering, Ritsumeikan University, Kusatsu, Shiga 525-8577, Japan.*
*E-mail: iwasakih@se.ritsumei.ac.jp*

Wavelength-modulated diffraction was developed by Iwasaki, Yurugi & Yoshimura [*Acta Cryst.* (1999), A**55**, 864–870] as a method for phase determination, in which the intensity of Bragg reflections is recorded using radiation whose wavelength is changing continually over a range in the vicinity of the absorption edge of an atom in the crystal. Using a ferrocene derivative crystal (chemical formula $C_{36}H_{32}O_7Fe$, space group $P2_1/a$) with the Fe atoms chosen as anomalous scatterers, measurements were made of the intensity gradient $dI/d\lambda$ of the reflections with an imaging plate as a detector on a synchrotron radiation source at Ritsumeikan University. In the case of a centrosymmetric crystal, the phase of the structure factor could be derived by measuring only the sign of $dI/d\lambda$ at one wavelength in the range. Of 104 reflections measured, the correct phase was assigned to 101 reflections. A discussion is given on the errors involved and on the limits of application of the method.

**Keywords: phase determination; anomalous scattering.**

## 1. Introduction

In a paper by Iwasaki *et al.* (1999), a new diffraction method was developed in which the intensity of Bragg reflections is recorded using radiation whose wavelength is changing continually over a range in the vicinity of the absorption edge of an atom in the crystal. If a two-dimensional detector such as an imaging plate is used, Bragg reflections appear as elongated spots, and the intensity gradient with respect to the wavelength measured on the plate contains information on the phase of the structure factor. With the intensity gradient measured at two different wavelengths and the positions of the anomalously scattering atoms known or properly assumed, the phase can be derived by solving simultaneous linear equations. The method, called the wavelength-modulated diffraction (WMD) method, is free from the problem of intensity scaling encountered when using other methods such as the multiwavelength diffraction method (*e.g.* Hendrickson, 1991).

The present paper reports the results of the application of the WMD method to the phase determination of a centrosymmetric crystal to test the feasibility. The theory developed by Iwasaki *et al.* (1999) shows that the procedure involved in the phase determination is particularly simple for that crystal, and knowing only the sign of the intensity gradient of the *hkl* reflection at one wavelength directly leads to the phase of $F(hkl)$. The errors involved and the application limits of the method are discussed.

## 2. Experimental

### 2.1. *Radiation for wavelength-modulated diffraction*

Owing to its wide continuous spectrum range, synchrotron radiation is most suited to WMD. At Ritsumeikan University a compact superconducting electron storage ring has been installed and, although the electron beam energy is not high (0.575 GeV), the radiation emitted from the ring of small radius (0.5 m) contains X-ray components that are usable for diffraction measurements (Iwasaki, Kurosawa *et al.*, 1998). At the beamline for X-ray diffraction, BL-1, a double-crystal monochromator of the Golovchenko-type (Golovchenko *et al.*, 1981) has been installed, which can provide a monochromatic radiation beam whose position is kept fixed even when the wavelength is continually changed.

The intensity of synchrotron radiation is, in general, dependent on the wavelength $\lambda$, and it is necessary to know the dependence prior to taking WMD measurements. The radiation spectrum of the compact superconducting ring is known, the intensity increasing with increasing wavelength in the X-ray range (Iwasaki, Nakayama *et al.*, 1998). In addition, the wavelength dependence of the reflecting power of the monochromator crystal and the beam-focusing mirror are to be known along with the wavelength dependence of the absorbing power of materials inserted into the incident-radiation beam path. However, what is required is the net wavelength dependence at the sample position $I_0(\lambda)$ and in the present study it was measured varying $\lambda$ continuously using the imaging-plate detector placed at that position. The dependence is almost linear and the intensity gradient, $dI_0/d\lambda$, is $0.44 \pm 0.02 \times 10^3\ \mathrm{nm}^{-1}$ around $\lambda$ = 0.175 nm, lower than expected from the radiation spectrum owing to absorption by beryllium foil.

### 2.2. *Sample crystal*

As a sample crystal, a ferrocene derivative crystal (chemical formula $C_{36}H_{32}O_7Fe$), synthesized by Nakamura & Setodoi (1998), was chosen. The *K*-absorption edge of the Fe atom (0.1743 nm) lies in the spectrum range most suitable to diffraction measurements at the compact superconducting ring. The crystal belongs to the monoclinic system with the centrosymmeric space group $P2_1/a$. The lattice parameters are $a$ = 0.7698 nm, $b$ = 1.0593 nm, $c$ = 3.649 nm and $\beta$ = 91.27°, four molecular units being contained in the unit cell. The sample crystal is plate-like, having approximate dimensions of 0.4 × 0.3 × 0.05 mm. The structure has been solved using the intensity data, collected using a four-circle X-ray diffractometer on a laboratory source, by the direct method (Nakamura & Setodoi, 1998), the final *R*-factor being 0.043.

### 2.3. *Recording of the wavelength-modulated diffraction pattern*

In order to obtain information on the phase of as many Bragg reflections as possible by the WMD method, the sample crystal is rotated while the monochromator crystals perform oscillatory rotations to change continuously the wavelength of the radiation in a definite range $\Delta\lambda$. Every reciprocal lattice point intersects the Ewald sphere of changing radius, but the intersection may not occur in the order of increasing or decreasing $\lambda$. It depends on the relative angular velocity of the two types of rotation and the geometrical position of the point in the reciprocal space. It is required that the point intersects the Ewald sphere of all the radii included in $\Delta\lambda$ so that an effective 'wavelength scan' of the reflection intensity is made. This requirement is met if the number of intersections is large and the monochromator crystal rotation is not synchronous with the sample crystal rotation. The 'random nature' of the intersections results in such a beneficial effect that a gradual change in the intensity of the primary radiation due to a finite lifetime of the stored electron beam is 'averaged out', and the intensity profile of the reflection recorded on the imaging plate is not affected by the intensity decay.

In the present study a conventional X-ray Weissenberg camera was first employed to record systematically Bragg reflections in the WMD

  

mode. It was originally designed to collect diffraction intensity data for radiation of a fixed wavelength, so that a modification would have to be made in order to vary the position of the layer-line screen synchronously with the change in λ. This problem was overcome by using the screen with a larger window width. WMD patterns were recorded with the [010]* axis chosen as the rotation axis. Δλ was set to be on the long-wavelength side of the *K*-absorption edge.

In the second stage of recording of Bragg reflections, a new diffraction apparatus was employed. It was designed and constructed on the basis of the Weissenberg camera mechanism (Koganezawa *et al.*, 2001), but has a larger camera radius (127.4 mm) and is equipped with an imaging-plate reader, which reads WMD patterns recorded on the plate automatically after exposure. Fig. 1 shows a pattern recorded using this apparatus with the layer-line screen removed, the rotation axis being the [010]* axis (vertical in the figure), as before. Δλ was set this time to be 0.1722–0.1797 nm in order to straddle the 0.1743 nm absorption edge, and the number of repetitions of the wavelength change was 104, although this number can be varied. It is seen that Bragg reflections appear elongated, the degree of elongation being dependent on various factors, as discussed by Greenhough *et al.* (1983), but it is, in general, larger for a reflection with a larger Bragg angle. The inset shows a magnified image of the $0\bar{2}15$ reflection. Another recording of the WMD pattern was made to cover a different region of the reciprocal space.

### 2.4. *Measurement of the intensity gradient and determination of the phase*

Of the Bragg reflections recorded, there are those for which the wavelength dependence of the intensity is clearly observed and those for which it is less recognizable. The $0\bar{2}15$ reflection belongs to the former group and its intensity profile recorded by the new apparatus is shown in Fig. 2, the intensity being expressed in arbitrary units. The profile has a dip at λ = 0.1740 nm and the intensity increases with increasing λ. The slight discrepancy between the position of the dip and that of the absorption edge (0.1743 nm) may be due to the chemical shift, the Fe atom being partly covalently and partly ionically bonded to the C atoms. The intensity gradient $dI/d\lambda$ is defined as the slope of the profile on the long-wavelength side of the edge, as shown by the solid line in the figure, yielding the value $1.65 \pm 0.04 \times 10^3$ nm$^{-1}$ for that reflection. The uncertainty arises from the non-smoothness of the profile, which is due to the deviation from randomness of the intersection of the reciprocal lattice point with the Ewald sphere and also to the finite pixel size of the imaging-plate reader. The measured gradient is rather large, but there are several reflections having a much larger intensity gradient.

Fig. 3 shows an intensity profile of the 201 reflection showing a negative slope on the long-wavelength side of the edge. It was obtained by the second recording of the pattern, in which Δλ was set to 0.1688–0.1768 nm. The expected intensity profile of this type of reflection is a peak at the absorption edge with a decrease on both sides. The slope is small and the intensity gradient has been measured to be $-1.02 \pm 0.06 \times 10^3$ nm$^{-1}$. The lower intensity on the short-wavelength side of the edge is due to increased sample absorption.

Measurements on a number of recorded reflections have shown that, whereas the number of reflections showing a positive intensity slope is large, the number of reflections with a negative slope is small and the magnitude of their $dI/d\lambda$ is small. The imbalance in the number arises partly from the wavelength dependence of the incident beam intensity and the observed profiles have been biased by $dI_0/d\lambda$. The reflections originally having a negative intensity gradient of magnitude smaller than $0.44 \pm 0.02 \times 10^3$ nm$^{-1}$ (the $dI_0/d\lambda$ value) appear to have a positive intensity slope. In addition, the relative contribution of the Fe atoms to the total structure factor determines the sign of $dI/d\lambda$, leading to the unbalanced numbers, as will be discussed below.

The practical way to correct the intensity gradient for the effect of $dI_0/d\lambda$ is to subtract its value from the observed one. For the reflections with intensity gradient magnitudes around that value, the error in the intensity gradient measurements may therefore be large. Needless to say, it is not possible to measure $dI/d\lambda$ for very weak

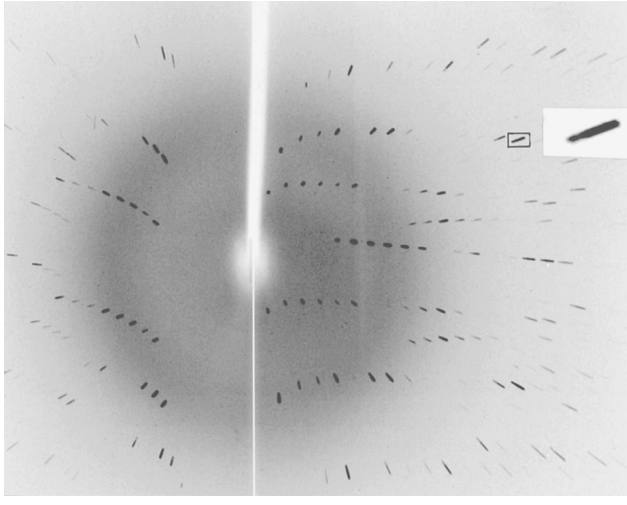

**Figure 1**
Wavelength-modulated diffraction pattern of a single crystal of $C_{36}H_{32}O_7Fe$, recorded using the new diffraction apparatus, based on the modified Weissenberg camera mechanism, on a 0.575 GeV synchrotron radiation source at Ritsumeikan University. The continually varied wavelength range was 0.1722–0.1797 nm, the *K*-absorption edge of Fe (free atom case) being at 0.1743 nm. The sample rotation axis is parallel to the [010]* direction and is in the vertical direction, while the rotation axis of the monochromator crystal is in the horizontal plane. The layer-line screen was removed. Bragg reflections appear elongated owing to the continual change in the wavelength of radiation. The inset shows a magnified image of the $0\bar{2}15$ reflection.

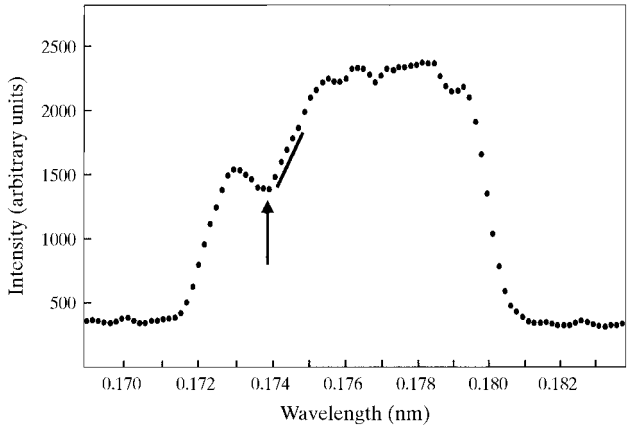


**Figure 2**
Intensity profile of the $0\bar{2}15$ reflection recorded in the wavelength-modulated diffraction mode using the new diffraction apparatus. The intensity is expressed in arbitrary units and the wavelength is expressed in nm. The dip in the profile indicates the position of the *K*-absorption edge, which is slightly different from that in the free atom case, 0.1743 nm, owing to the bonding effect (chemical shift). The intensity gradient is defined as a slope on the long-wavelength side of the absorption edge.

reflections and also for reflections lying in the low Bragg angle region which have a small degree of elongation.

According to Iwasaki *et al.* (1999), the intensity gradient of an *hkl* reflection for a centrosymmetric crystal is expressed as

$$\partial I(hkl)/\partial\lambda = 2(\partial f'_H/\partial\lambda)\left(\textstyle\sum_H \cos\theta_H\right)F(hkl), \qquad (1)$$

where $f'_H$ is the real part of the anomalous scattering factor of the heavy atom, the Fe atom in the present case. $\sum_H \cos\theta_H$ represents the sum of $\cos 2\pi(hx_j + ky_j + lz_j)$, where $x_j$, $y_j$ and $z_j$ are the coordinates of the heavy atoms and the sum is taken for all of them. We use (1) to derive the phase of $F(hkl)$. Then, there is no need to know the magnitude of the sum, only its sign. $\partial f'_H/\partial\lambda$ is always positive on the long-wavelength side of the absorption edge and for the reflection with the positive sign of the sum the phase of $F(hkl)$ is 0 when $\partial I(hkl)/\partial\lambda$ is positive and $\pi$ when it is negative. Determination of the phase is thus simple for the centrosymmetric crystal.

In the ferrocene derivative crystal there are four Fe atoms, whose positions were determined by Nakamura & Setodoi (1998), but attempts have been made here to determine them from the Patterson map synthesized using their intensity data. The sum of $\cos 2\pi(hx_j + ky_j + lz_j)$ was then calculated and its sign was obtained for the reflections recorded.

Table 1 lists the phase of the structure factor determined in this way for the crystal. The list does not include the reflections for which the intensity gradient could not be measured. For comparison, the phases calculated from the coordinates of the atoms, except for the H atoms, determined by Nakamura & Setodoi (1998), are also listed. There are 104 reflections in total, of which 101 have been given the phase in agreement with the phase calculated. The discrepancy for the other three reflections is due to the error in measuring the intensity gradient.

As Table 1 shows, there is an approximately equal number of reflections with phase 0 and phase $\pi$. It is to be noted that this does not necessarily mean that the number of reflections with a positive and a negative intensity gradient is approximately the same. Simple calculation has shown that the negative sign of $dI/d\lambda$ is associated only with the reflections in which the Fe atoms do not dominate $F(hkl)$, and the sign of the partial structure factor of these atoms is opposite to the sign of that of the other atoms. The number of reflections with a negative intensity gradient is thus about one-quarter of the total number of reflections and, moreover, the negative gradient reflections have low or medium intensities.

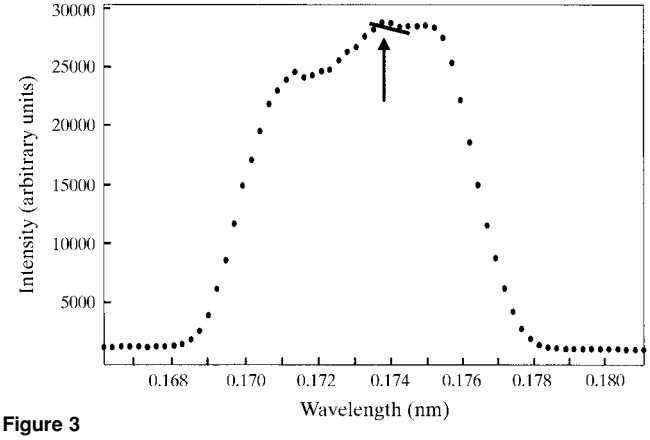


**Figure 3**
Intensity profile of the 201 reflection recorded again, with the new apparatus, in which $\Delta\lambda$ was set to 0.1688–0.1768 nm. The absorption edge is at the peak position, indicated by the arrow, and the intensity gradient is negative on the long-wavelength side.

Equation (1) may also be used to determine the magnitude of $F(hkl)$, if $\partial I(hkl)/\partial\lambda$ is measured in absolute units. It is, however, practical to obtain it from a separate integrated intensity measurement employing a four-circle X-ray diffractometer or other conventional X-ray diffraction apparatus and assign the phase obtained by the WMD method to $\left|F(hkl)\right|$ for the synthesis of an electron density map.

## 3. Discussion

### 3.1. *Errors in the determination of the phase*

Possible errors which may be introduced in the phase determination by the WMD method are: those in the measurement of the intensity gradient from the Bragg reflection profile; those arising from the wavelength dependence of the incident beam intensity; and those arising from the uncertainty of the coordinates of the anomalous scatterers. They are discussed in order below.

The intensity profile of Bragg reflections is obtained by the intersection of the reciprocal lattice points with the Ewald sphere of changing radius. Although the number of repetitions of the wavelength change was taken to be larger than 100 in the present study, there still remains a deviation from the randomness of the intersection, resulting in a rough intensity profile and an assignment of wrong phases to several reflections. Even though the number of repetitions is increased, the finite pixel size of the imaging-plate reader is another origin of the roughness in the profile. It is desirable, therefore, to record Bragg reflections changing $\lambda$ with a larger number of repetitions and using a 'camera' of a larger radius for them to appear as larger elongated spots. This, however, requires an unreasonably longer exposure time in some cases. The quality of the sample crystal also has an influence on the profile and an error may be introduced if it shows ill-defined Bragg reflections, though an intermediate case of finite mosaicity may smooth out the effect. The wavelength dependence of absorption by the sample crystal containing an increased number of anomalous scatterers may have an influence on the intensity gradient, even on the long-wavelength side of the edge. In the present case of the ferrocene derivative crystal, the effect is less significant than the effect of $dI_0/d\lambda$ and has been neglected.

An alternative way of recording a Bragg reflection profile was proposed by Arndt *et al.* (1982), in which the radiation of a band of wavelengths produced by reflection by a bent-crystal monochromator was used. It would give a smoother intensity profile in the WMD pattern and make measurement of the intensity gradient easier. The incident beam, however, is not a parallel beam and another kind of dispersion would be introduced into the profile, making derivation of $dI/d\lambda$ somewhat complicated, although an elaborate analysis of the profile was made by Greenhough *et al.* (1983).

An ideal radiation source for the WMD measurements is one which emits radiation of an intensity that is independent of wavelength. The spectrum of the radiation from the bending magnet in a high-energy ring, such as SPring-8, has an almost flat range in the X-ray region and is most suited. At the compact superconducting ring, the wavelength dependence of the primary beam intensity is appreciable and due correction has to be made on the measured intensity gradient. It is possible, however, to adjust the spectrum by inserting appropriate materials into the radiation beam path, as shown above, at the expense of loss in the photon flux.

For any method of phase determination using the anomalous scattering phenomenon, knowledge of the coordinates of the anom-

**Table 1**
List of the phase $\varphi_0(hkl)$ of Bragg reflections of a $C_{36}H_{32}O_7Fe$ crystal (space group $P2_1/a$) determined by the wavelength-modulated diffraction method.

For comparison, the phases $\varphi_c(hkl)$ calculated from the atomic coordinates determined by Nakamura & Setodoi (1998) are listed. In the $|F(hkl)|$ column, the structure factor values measured by Nakamura & Setodoi (1998) are listed.

| *hkl* | $\|F(hkl)\|$ | $\varphi_0(hkl)$ | $\varphi_c(hkl)$ | *hkl* | $\|F(hkl)\|$ | $\varphi_0(hkl)$ | $\varphi_c(hkl)$ |
|---|---|---|---|---|---|---|---|
| 006 | 210.1 | π | π | $\bar{1}11$ | 79.8 | π | π |
| 007 | 178.9 | π | π | $\bar{1}110$ | 42.8 | π | π |
| 008 | 157.7 | π | π | $\bar{1}19$ | 86.0 | π | π |
| 009 | 105.9 | π | π | $\bar{1}18$ | 57.6 | π | π |
| 0010 | 79.1 | π | π | $\bar{1}17$† | 67.8 | π | 0 |
| 0012 | 14.1 | π | π | $\bar{1}16$ | 30.2 | π | π |
| 0013 | 81.8 | 0 | 0 | $\bar{1}1\bar{3}$ | 105.4 | π | π |
| 0016 | 123.3 | 0 | 0 | $\bar{1}1\bar{4}$ | 58.9 | π | π |
| 0017 | 110.8 | π | π | $\bar{1}1\bar{5}$ | 144.1 | π | π |
| $\bar{2}021$ | 86.1 | 0 | 0 | $\bar{1}1\bar{6}$ | 124.3 | π | π |
| $\bar{2}020$ | 98.0 | 0 | 0 | $\bar{1}1\bar{7}$ | 114.6 | π | π |
| $\bar{2}017$ | 82.6 | 0 | 0 | $\bar{1}1\bar{8}$ | 42.3 | π | π |
| $\bar{2}016$ | 95.0 | π | π | $\bar{1}1\bar{9}$ | 47.3 | 0 | 0 |
| $\bar{2}014$ | 82.4 | π | π | $\bar{1}1\bar{1}0$ | 100.7 | 0 | 0 |
| $\bar{2}012$ | 44.2 | π | π | $\bar{1}1\bar{1}\bar{1}$ | 72.7 | 0 | 0 |
| $\bar{2}011$ | 107.7 | π | π | $\bar{1}1\bar{1}\bar{2}$ | 58.3 | 0 | 0 |
| $\bar{2}08$ | 44.2 | 0 | 0 | $\bar{1}1\bar{1}\bar{3}$ | 62.2 | 0 | 0 |
| $\bar{2}06$ | 75.2 | 0 | 0 | $\bar{1}1\bar{1}\bar{4}$ | 39.9 | 0 | 0 |
| $\bar{2}05$ | 108.8 | 0 | 0 | $\bar{1}1\bar{1}\bar{6}$ | 55.3 | π | π |
| $\bar{2}04$ | 65.3 | 0 | 0 | $\bar{2}18$ | 50.8 | 0 | 0 |
| $\bar{2}03$ | 75.2 | π | π | $\bar{2}17$ | 77.8 | π | π |
| $\bar{2}01$ | 41.9 | π | π | $\bar{2}14$ | 70.4 | π | π |
| $\bar{2}0\bar{1}$‡ | 292.1 | π | 0 | $\bar{2}12$ | 65.8 | π | π |
| $\bar{2}0\bar{2}$ | 352.5 | π | π | $\bar{2}11$ | 61.7 | π | π |
| $\bar{2}0\bar{3}$ | 49.9 | π | π | $\bar{2}1\bar{1}$ | 119.2 | 0 | 0 |
| $\bar{2}0\bar{7}$ | 44.3 | 0 | 0 | $\bar{2}1\bar{2}$ | 26.6 | 0 | 0 |
| $\bar{2}0\bar{8}$ | 122.5 | 0 | 0 | $\bar{2}1\bar{4}$ | 156.0 | 0 | 0 |
| $\bar{2}0\bar{1}0$ | 132.5 | 0 | 0 | $\bar{2}1\bar{5}$ | 39.2 | 0 | 0 |
| $\bar{2}0\bar{1}\bar{7}$ | 101.2 | π | π | $\bar{2}1\bar{6}$ | 42.1 | π | π |
| $\bar{2}0\bar{1}\bar{8}$ | 178.6 | π | π | $\bar{2}1\bar{7}$† | 47.1 | 0 | π |
| $\bar{4}017$ | 80.1 | π | π | $\bar{2}1\bar{8}$ | 77.5 | 0 | 0 |
| $\bar{4}016$ | 83.2 | π | π | $\bar{2}1\bar{9}$ | 32.4 | π | π |
| $\bar{4}014$ | 71.5 | 0 | 0 | $\bar{2}1\bar{1}\bar{1}$ | 54.5 | π | π |
| $\bar{4}010$ | 164.6 | 0 | 0 | $\bar{2}1\bar{1}\bar{2}$ | 36.6 | 0 | 0 |
| $\bar{4}04$ | 108.1 | π | π | $\bar{3}118$ | 69.4 | π | π |
| $\bar{4}02$ | 82.5 | π | π | $\bar{3}116$ | 117.6 | π | π |
| $\bar{4}0\bar{2}$ | 92.0 | π | π | $\bar{3}115$ | 112.6 | π | π |
| $\bar{4}0\bar{4}$ | 90.2 | π | π | $\bar{3}114$ | 103.9 | π | π |
| $\bar{4}0\bar{5}$ | 76.1 | π | π | $\bar{3}113$ | 60.1 | π | π |
| $\bar{4}0\bar{7}$ | 84.0 | π | π | $\bar{3}110$ | 62.0 | 0 | 0 |
| $\bar{4}0\bar{1}0$ | 109.1 | π | π | $\bar{3}19$ | 101.6 | 0 | 0 |
| $\bar{4}0\bar{1}\bar{2}$ | 193.3 | π | π | $\bar{3}17$ | 70.1 | 0 | 0 |
| 0117 | 76.8 | π | π | $\bar{3}16$ | 44.5 | 0 | 0 |
| 0116 | 68.9 | 0 | 0 | $\bar{3}15$ | 31.6 | π | π |
| 0111 | 85.4 | 0 | 0 | $\bar{3}11$ | 58.0 | π | π |
| 0110 | 51.4 | π | π | $\bar{3}10$ | 135.7 | π | π |
| 019 | 22.7 | π | π | $\bar{3}1\bar{5}$ | 127.2 | 0 | 0 |
| 016 | 45.8 | 0 | 0 | $\bar{3}1\bar{6}$ | 68.8 | 0 | 0 |
| 015 | 24.6 | π | π | $\bar{3}1\bar{7}$ | 70.9 | 0 | 0 |
| 014 | 36.2 | 0 | 0 | $\bar{3}1\bar{1}\bar{2}$ | 90.8 | π | π |
| $\bar{1}117$ | 35.4 | 0 | 0 | $\bar{3}1\bar{1}\bar{4}$ | 97.1 | π | π |
| $\bar{1}112$ | 45.9 | π | π | $0\bar{2}15$ | 156.4 | 0 | 0 |

‡ This is a rather strong reflection but a rough intensity profile led to the wrong phase. Remeasurement for the symmetry-related reflection, 201, in the second recording using the new apparatus with a different range $\Delta\lambda$, shown in Fig. 3, resulted in the asssignment of the correct phase. † This is a weak reflection with a rough intensity profile.

alously scattering atoms is a prerequisite to solving the problem. The accuracy with which they are known depends on the number and arrangement of those atoms. In the phase determination for centrosymmetric crystals by the WMD method, however, what is required is the sign of the sum $\sum_H \cos\theta_H$, and the error in the sign arising from the uncertainty of the coordinates is smaller than the error in the magnitude of the sum. The effect is appreciable only for reflections with a sum of small magnitude and they are not, in general, strong reflections. In the present study, the atomic coordinates of the Fe atoms could be rather unequivocally derived from the Patterson map and were in agreement to three decimal places with those refined in the ordinary structure analysis (Nakamura & Setodoi, 1998) for most of the reflections.

### 3.2. *Application of the WMD method*

The WMD method will be successfully applied to crystals consisting of a majority of light atoms and a minority of heavy atoms, thereby the effect of anomalous scattering of the latter atoms being appreciable. The possible range of anomalous scatterers in the *shy;periodic table is $Z$ = 20–29 for the $K$-absorption edge, if the measurements are made at the compact superconducting ring. Likewise, for the $L$-absorption edge the range is $Z$ = 48–65 . The range can be extended to a larger atomic number at the high-energy rings. The number of Bragg reflections to which the phases are assigned is dependent of the wavelength used and it is advantageous to use anomalous scatterers of larger atomic number. Judging from the results of the present study, the lower limit of the concentration of the anomalous scatterers is around 10% in the mass-fraction for the $K$-absorption edge ($\partial f'_H/\partial\lambda$ being approximately $8e^-/0.001$ nm). Since the WMD method is a method of intensity profile analysis, sample crystals which do not show a smooth profile of Bragg reflections cannot be used.

The concept of phase determination by multiwavelength anomalous diffraction has a long history (*e.g.* see Okaya & Pepinsky, 1956) and recently Hendrickson (1991) developed it into the so-called MAD method, which has been extensively used, particularly for macromolecular crystallography. Multiwavelength anomalous diffraction is beginning to find application in chemical crystallography (see Helliwell *et al.*, 1999). Based on the integrated intensity data, MAD determines the phase and finally leads to a possible structure model. In this sense it is regarded as one of the 'complete' methods of structure analysis, but the data are collected at several wavelengths and intensity scaling can be a problem. WMD, on the other hand, is free from this problem, but works only as a method for the phase determination. It is to be noted, however, that WMD enables one to the visualize the *phase* of Bragg reflections as a slope of the intensity profile and to make a judgement on whether the assigned phases are reliable or not.

For crystals containing atoms whose atomic number is close to that of the anomalous scatterers, phase determination is also possible, provided that the coordinates of those atoms are known in addition to those of the anomalous scatterers, as treated theoretically by Iwasaki *et al.* (1999).

The authors express thanks to Dr K. Handa and Mr M. Kato for their assistance in the X-ray diffraction experiments. The present work has been supported in part by the High Technology Research Project of the Ministry of Education, Science and Culture.

### References

Arndt, U. W., Greenhough, T. J., Helliwell, J. R., Howard, J. A. K., Rule, S. A. & Thompson, A. W. (1982). *Nature (London)*, **298**, 835–838.
Golovchenko, J. A., Levesque, R. A. & Cowan, P. L. (1981). *Rev. Sci. Instrum.* **52**, 509–516.
Greenhough, T. J., Helliwell, J. R. & Rule, S. A. (1983). *J. Appl. Cryst.* **16**, 242–250.
Helliwell, M., Helliwell, J. R., Kaucic, V., Zabukovec Logar, N., Barba, L., Busetto, E. & Lausi, A. (1999). *Acta Cryst.* B**55**, 327–332.
Hendrickson, W. A. (1991). *Science*, **254**, 51–58.
Iwasaki, H., Kurosawa, N., Masui, S., Fujita, S., Yurugi, T., Yoshimura, Y. & Nakamura, N. (1998). *J. Synchrotron Rad.* **5**, 333–335.

Iwasaki, H., Nakayama, Y., Ozutsumi, K., Yamamoto, Y., Tokunaga, Y., Saisho, H., Matsubara, T. & Ikeda, S. (1998). *J. Synchrotron Rad.* **5**, 1162–1165.
Iwasaki, H., Yurugi, T. & Yoshimura, Y. (1999). *Acta Cryst.* A**55**, 864–870.
Koganezawa, T., Handa, K., Nakamura, N., Yoshimura, Y., Iwasaki, H., Yamada, T. & Shoji, T. (2001). *Nucl. Instrum. Methods*. In the press.
Nakamura, N. & Setodoi, S. (1998). *Mol. Cryst. Liq. Cryst.* **319**, 173–181.
Okaya, Y. & Pepinsky, R. (1956). *Phys. Rev.* **103**, 1645–1647.


Received 28 August 2000 • Accepted 19 March 2001